
OPTIMISATION OF LARGE WAVE FARMS USING A MULTI-STRATEGY EVOLUTIONARY FRAMEWORK

A PREPRINT

Mehdi Neshat

Optimization and Logistics Group
School of Computer Science
The University of Adelaide
Australia
mehdi.neshat@adelaide.edu.au

Bradley Alexander

Optimization and Logistics Group
School of Computer Science
The University of Adelaide
Australia
bradley.alexander@adelaide.edu.au

Nataliia Y. Sergiienko

School of Mechanical Engineering
The University of Adelaide
Australia
nataliia.sergiienko@adelaide.edu.au

Markus Wagner

Optimization and Logistics Group
School of Computer Science
The University of Adelaide
Australia
markus.wagner@adelaide.edu.au

March 24, 2020

ABSTRACT

Wave energy is a fast-developing and promising renewable energy resource. The primary goal of this research is to maximise the total harnessed power of a large wave farm consisting of fully-submerged three-tether wave energy converters (WECs). Energy maximisation for large farms is a challenging search problem due to the costly calculations of the hydrodynamic interactions between WECs in a large wave farm and the high dimensionality of the search space. To address this problem, we propose a new hybrid multi-strategy evolutionary framework combining smart initialisation, binary population-based evolutionary algorithm, discrete local search and continuous global optimisation. For assessing the performance of the proposed hybrid method, we compare it with a wide variety of state-of-the-art optimisation approaches, including six continuous evolutionary algorithms, four discrete search techniques and three hybrid optimisation methods. The results show that the proposed method performs considerably better in terms of convergence speed and farm output.

Keywords Wave Energy Converters · Large wave farm · Optimisation · Evolutionary Algorithms · Hybrid multi-strategy evolutionary method · Discrete local search.

1 Introduction

The use of renewable energy sources continues to exhibit very fast growth of deployment, and it has resulted in savings of more than two gigatonnes of carbon dioxide in 2018 alone [1]. One of the most promising renewable sources is ocean wave energy, which has a high energy density per unit area of ocean, high level of predictability, and potentially high capacity factors [2, 3]. However, compared to wind and solar energy, wave energy is still a nascent field, and research is still very active converter design [4], wave-farm layout, and power-take-off parameters [5, 6].

While there has been significant research on the placement of wave energy converters (WECs) in farms [7, 8, 9, 10, 11], to date, only Wu et al. [9] has considered the design of larger layouts of over 20 converters, using a much-simplified wave energy model.

The research described in this paper extends previous work by using a much more detailed energy model to place buoys in large farms of up to 100 WECs. Due to the much higher number of interactions modelled in such farms this work requires the development of novel, specialised, and highly-efficient search heuristics. Using an improved energy model, we demonstrate the performance of these new algorithms in two contrasting real wave scenarios (Sydney and Perth) and compare their performance to a suite of extant optimisation algorithms.

This paper is organised as follows. In the next section, we survey related work. Section 3 describes our WEC model. Section 4 formulates the optimisation problem. The proposed optimisation methods are described in Section 5. The results of the optimisation experiments, including simple landscape analysis, are described in Section 6. Section 7 concludes this paper and canvases future work.

2 Related Work

Placement of WECs in larger farms is a challenging optimisation problem. Hydrodynamic interactions between WECs are complex, which makes evaluation of each potential layout time-consuming [10], ranging from minutes to hours for large farms. Second, due to complex inter-WEC interactions, the search space for this problem is multi-modal – thus requiring global search to be assured of good results. Finally, the high number of decision variables in large farms increases the search space to traverse.

There has been substantial past research into the problem of WEC placement. One of the first studies to optimise WEC layout compared a customised genetic algorithm (GA) with an iterative Parabolic Intersection (PI) method [7] for a small wave farm (five buoys). The GA outperformed PI, but required more evaluations to do so. A more recent position optimisation study [8] compared three search metaheuristics: a custom GA, CMA-ES [12], and glow-worm optimisation [13]), using a simple wave model. The study observed that CMA-ES converges the fastest, while the other models produced slightly better results. Wu et al. [9] considered optimising a large wave farm (25–100 WECs) as an array of fully submerged three-tether buoys using 1+1EA and 2+2CMA-ES. That research found that the 1+1EA

with a simple mutation operator performed better than CMA-ES. A limitation of that work was that it was limited to a highly simplified single-wave-direction wave scenario.

In a move toward problem-specific algorithms, Neshat et al. [10] proposed a hybrid optimisation method (LS-NM) combined with a neighbourhood search and Nelder-Mead search. Their study found that LS-NM performed better than generic and custom EAs. However, the wave model applied by that study, though quite detailed, still used an artificial wave scenario and small farm sizes (4 and 16 WECs). More recently, more problem-specific search techniques [11, 14] were, respectively, proposed for optimising WECs positions by utilising a surrogate power model (that is learned on the fly); and hybrid symmetric local search by defining a search sector to speed up the optimisation process. These approaches were also applied to real wave scenarios. For handling this real expensive optimisation problem, a neuro-surrogate optimisation approach was recommended [15] that is composed of a surrogate Recurrent Neural Network (RNN) model and a symmetric local search. This surrogate model is joined with a metaheuristic (Gray Wolf optimiser) for tuning the models hyper-parameters. However, these search strategies performance were not evaluated on a large farm.

This article differs from previous work by optimising large layouts using an improved high-fidelity hydrodynamic model to optimise layouts in real wave scenarios. We develop a new hybrid multi-strategy evolutionary algorithm for optimising the positions of buoys in the wave farm to maximise the average total farm power output. For evaluating the new algorithm, we compare its performance to: (1) six continuous off-the-shelf evolutionary methods, (2) four discrete heuristic approaches (3 new), population and individual-based, and (3) three new hybrid EAs (continuous+discrete). We use these methods to optimise wave farms of sizes 49 and 100. We use fine-grained models of contrasting real wave climates, Perth and Sydney, which are located off the southern coast of Australia. The optimisation results demonstrate that the new hybrid multi-strategy search approach produces the best results.

3 The wave energy converter model

This section describes the energy model for WEC layouts used in this study. The WEC design simulated here is a three-tether spherical buoy based on the highly effective CETO 6 system developed by Carnegie Clean Energy [16].

3.1 Equation of motion

We model a fully submerged spherical buoy of 5 m radius that is tethered to three power take-off units installed on a seabed. A detailed description of this WEC and its physical parameters can be found in [10].

The motion of each buoy in the farm depends on the forces due to the fluid-structure interaction and the force exerted on the buoy from the PTO system. The generalised equation that describes the motion of all buoys can be written in the frequency domain as:

$$(\mathbf{M} + \mathbf{A})\ddot{\mathbf{X}} + (\mathbf{B} + \mathbf{D}_{pto})\dot{\mathbf{X}} + \mathbf{K}_{pto}\mathbf{X} = \mathbf{F}_{exc}, \quad (1)$$

where $\mathbf{X} \in \mathbb{R}^{3N \times 1}$ is a vector of surge, sway and heave displacements of each buoy, $\mathbf{M} = m\mathbb{I}_{3N}$ is a diagonal mass matrix of the wave farm, \mathbf{A} and $\mathbf{B} \in \mathbb{R}^{3N \times 3N}$ are the matrices of hydrodynamic added mass and damping coefficients respectively, \mathbf{K}_{pto} and $\mathbf{D}_{pto} \in \mathbb{R}^{3N \times 3N}$ are the block diagonal matrices of PTO stiffness and damping coefficients respectively, and $\mathbf{F}_{exc} \in \mathbb{R}^{3N \times 1}$ is a vector of excitation forces.

3.2 Performance assessment

After solving the equation of motion (1), we can calculate the power absorbed by the farm in a regular wave of frequency ω that propagates from direction β :

$$p(\omega, \beta) = \frac{1}{2} \dot{\mathbf{X}}^* \mathbf{D}_{pto} \dot{\mathbf{X}} \quad (2)$$

where $()^*$ denotes the conjugate transpose of a matrix.

Eq. (2) allows us to estimate the power production of a farm assuming that the ocean wave has only one frequency component (like a sinusoidal wave) and propagates only from one direction. In reality, ocean waves travel from different directions and contain multiple frequencies. This behaviour of the wave is usually described by the directional wave spectrum $S(\omega, \beta)$, and power generated by the wave farm in the irregular wave, or sea state (H_s, T_p) , can be approximated by:

$$P(H_s, T_p) = \int_0^{2\pi} \int_0^\infty S(\omega, \beta) p(\omega, \beta) d\omega d\beta. \quad (3)$$

A potential deployment site (e.g. Perth or Sydney) can be characterised by the wave climate where each sea state has the probability of occurrence $O(H_s, T_p)$. Therefore, using values from Eq. (3) and having historical wave climate statistics, it is possible to calculate the annual average power generated by the wave farm at a given location:

$$P_\Sigma = \sum P(H_s, T_p) O(H_s, T_p). \quad (4)$$

The Perth and Sydney sites are qualitatively very different: Perth has a small sector from which the prevailing waves arrive, while Sydney's wave directions vary much more. For Perth, this can result in very pronounced constructive and destructive interference, while the same are "smeared" out for Sydney, thus resulting in two very different optimisation scenarios.

Another metric that is widely used to demonstrate the quality of the buoy placement in a farm is called the q -factor. It can be calculated as a ratio of the power generated by the entire farm P_Σ to the sum of power outputs from all WECs if they operate in isolation (not in a farm) P_Σ^i :

$$q = \frac{P_\Sigma}{\sum_i^N P_\Sigma^i} \quad (5)$$

Values of $q > 1$ indicate that this particular farm benefits from the constructive interaction between WECs, and more energy can be generated if these WECs operate together.

The MATLAB implementation of this model can be downloaded at [17].

4 Optimisation problem formulation

Based on our WEC model, the problem of positioning N converters on a restricted area of a wave farm ($l \times w$) in order to maximise the average annual power production P_Σ is:

$$P_\Sigma^* = \operatorname{argmax}_{\mathbf{x}, \mathbf{y}} P_\Sigma(\mathbf{x}, \mathbf{y})$$

where $P_\Sigma(\mathbf{x}, \mathbf{y})$ is the average power obtained by placements of the buoys in a field at x -positions $\mathbf{x} = [x_1, \dots, x_N]$ and corresponding y positions $\mathbf{y} = [y_1, \dots, y_N]$. In our experiments, the number of buoys is $N = 49$ and 100 .

Constraints All buoy positions (x_i, y_i) are constrained to a square field of dimensions: $l \times w$ where $l = w = \sqrt{N * 20000} m$. This allocates $20000m^2$ of farm-area per-buoy. In addition, the intra-buoy distance must not be less than 50 meters for reasons of safety and maintenance access. For any layout \mathbf{x}, \mathbf{y} the sum-total of the inter-buoy distance violations, measured in metres, is:

$$\begin{aligned} Sum_{dist} = \sum_{i=1}^{N-1} \sum_{j=i+1}^N (dist((x_i, y_i), (x_j, y_j)) - 50), \\ \text{if } dist((x_i, y_i), (x_j, y_j)) < 50 \text{ else } 0 \end{aligned}$$

where $dist((x_i, y_i), (x_j, y_j))$ is the Euclidean distance between each pair of buoys i and j .

Violations of the inter-buoy distance constraint are handled by applying a steep penalty function: $(Sum_{dist} + 1)^{20}$ and then applying the Nelder-Mead simplex algorithm over this penalty function to repair the violations in the layout. This approach avoids expensive re-evaluations of the full-wave model that would be required if the penalty function were combined with the full model whilst repairing distance violations. Meanwhile, we handle buoy placements outside of the farm area by moving them back to the farm boundary.

Computational Resources In this paper, we aim to compare several heuristic search methods, for 49 and 100-buoy layouts, in two realistic wave models. Because the search methods apply the interaction model to differing numbers of buoys at a time, it is not feasible to compare methods fairly in terms of a fixed number of model evaluations.

Instead, we use an allocated time budget for each run of three days on dedicated nodes of an HPC platform with 2.4GHz Intel 6148 processors and 128GB of RAM. The software environment running the function evaluations and the search algorithms is MATLAB R2019. On this platform, 12-fold parallelisation inside of Matlab yields up to 10-fold speedup. All algorithm variants are carefully implemented to make use of the parallelism available.

5 Optimisation Methods

The algorithms that follow apply three broad strategies. In the first strategy, we optimise in a continuous space using five off-the-shelf evolutionary algorithms. We also use the LS-NM [10] algorithm, which places and fine-tunes one

buoy at a time. In the second strategy, we optimise the positions in a discretised grid where the spacing is based on the safety-distance. Here, we consider four different EAs.

Last, we propose a hybrid multi-strategy heuristic that is designed based on our observations that attempts to combine the strengths of the algorithms from the first two strategies.

5.1 Continuous methods

For the continuous optimisation strategy, we compare six meta-heuristic approaches to optimise all problem dimensions simultaneously:

1. covariance matrix adaptation evolutionary-strategy (CMA-ES) [12, 18] which is an state-of-the-art and self-adaptive EA with the default $\lambda = 12$, and initial $\sigma = 0.25 \times (U_b - L_b)$;
2. (2+2)CMA-ES [9] with the default $\lambda = 2$, and $\sigma = 0.3 \times (U_b - L_b)$;
3. Differential Evolution (DE) [19], a well known global search heuristic using a binomial crossover and a mutation operator of *DE/rand/1/bin*. The population size is adjusted by the $\lambda = 12$ and other control parameters are $F = 0.5$, $P_{cr} = 0.8, 0.9$ respectively for 49 and 100-buoy layouts;
4. Improved Differential Evolution [20], with $\lambda = 12$, and generating mutation vector in the form of *DE/best/1/bin* with an adaptive mutation operator $F = F_0 \times 2^{e^{-\frac{G_m}{\sigma_{m+1}-G}}}$, where $F_0 = 0.5$ and G_m is the maximum number of generations and G is the current generation;
5. a simple (1+1)EA as used in [9] that mutates one buoy location in each iteration with a probability of $1/N$ using a normal distribution ($\sigma = 0.1 \times (U_b - L_b)$);
6. Local Search + Nelder-Mead (LS-NM) [10]: which is a fast and effective WEC position optimisation method. Each buoy is placed and optimised one-at-a-time sequentially by sampling at a normally-distributed random offset ($\sigma = 70m$) from the earlier placed buoy position. The sampled position proffering the highest power output, after NM search, is taken.

5.2 Discrete methods

We test and compare four discrete optimisation methods. All methods place buoys at locations on a grid spaced at the safety distance of 50m. A-priori this discretisation offers advantages in terms of avoiding infeasible layouts and reduced overall search space.

The discrete algorithms used here are:

1. binary Genetic Algorithm (bGA) [21] with $\lambda = 12$, $e_p = 10\%$, $C_r = 80\%$, $M_r = 10\%$, a binary mutation and double point crossover with respect to the number of buoys as a constraint, where e_p , C_r and M_r are the elitism, crossover and mutation rate respectively.

2. Improved binary Differential Evolution (bDE) [22] with the same IDE settings and to construct the mutant vector, formula 6 and 7 are used;

$$Diff - Vector^j = \begin{cases} 0, & if(X_{r_1}^j = X_{r_2}^j) \\ X_{r_1}^j, & otherwise \end{cases} \quad (6)$$

$$Mutant - Vector^j = \begin{cases} 1, & if(Diff - Vector^j = 1) \\ X_{G_{best}}^j, & otherwise \end{cases} \quad (7)$$

where r_1 and r_2 are the index of two randomly chosen individuals, and G_{best} mentions the best solution number in the current population.

3. Enhanced binary Particle Swarm Optimisation (bPSO) [23, 24] with $\lambda = 12$, and other settings are $C_1 = C_2 = 2$, $\omega_{ini} = 2$, $\omega_{max} = 0.9$, $\omega_{min} = 0.4$, and ω is linearly decreased to 1.5. the applied transfer function (V-shaped) is represented by Equation 8 and the position vector is updated by Equation 9.

$$T(v_i^k(t)) = \left| \frac{2}{\pi} \arctan\left(\frac{\pi}{2} v_i^k(t)\right) \right| \quad (8)$$

$$X_i^k(t+1) = \begin{cases} (X_i^k(t))^{-1} & if \text{ rand} < T(v_i^k(t)) \\ X_i^k(t) & otherwise \end{cases} \quad (9)$$

where $v_i^k(t)$ indicates the i^{th} particle velocity at iteration t in the k^{th} dimension.

4. Discrete Local Search (DLS), which is an individual-based evolutionary algorithm similar to a $1 + 1EA$ with two kinds of mutation step sizes: one discrete interval based on a uniform random distribution that can be vertical, horizontal or diagonal with the same probability, and using a discrete normally-distributed random offset with $\sigma = 3$ (DLS(II)). The mutation probability rate is $\frac{1}{N}$, where N is the number of buoys. In DLS(II), we first generate an initial population, and then the best arrangement is chosen as a start individual.

5.3 Hybrid methods

In the third strategy, we proposed a hybrid heuristic framework which consists of five steps:

- **First step:** Applying Symmetric Local Search + Nelder-Mead (SLS-NM) [14]: which places one buoy at a time but offers a more systematic local search. The search starts by placing the first buoy in a pre-determined position of the field based on the dominant wave direction; a symmetric sampling around the neighbourhood of the current buoy is done. Next, Nelder-Mead is applied to optimise the placed buoy arrangement concerning the continuous variables. This process is repeated until the last buoy is placed. In our present case, we use SLS-NM to optimise a local 4-buoy sub-layout which will act as a surrogate layout model. Restricting the

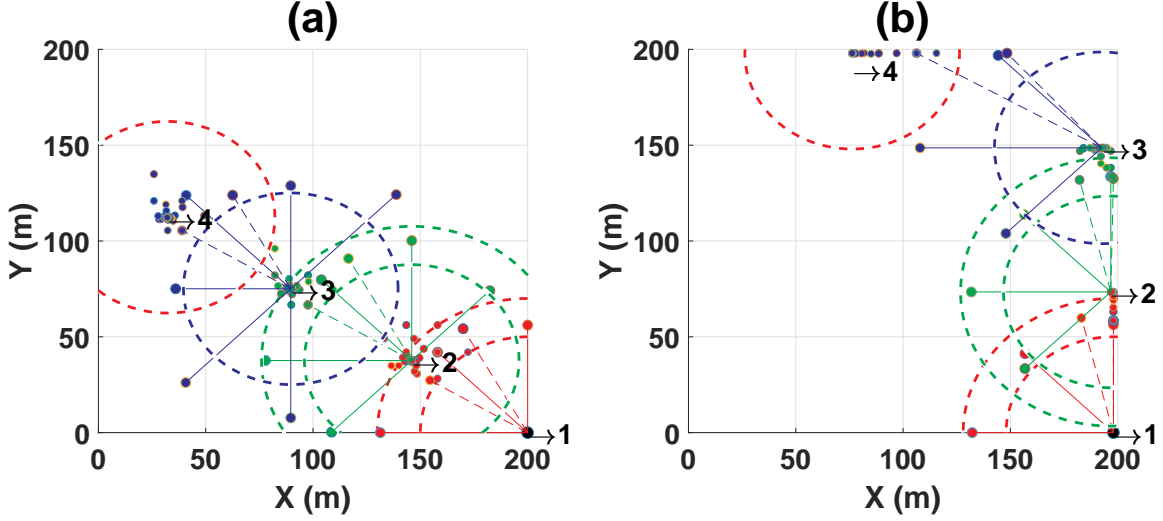


Figure 1: Symmetric Local Search + Nelder-Mead (SLS-NM) [14] for making the surrogate model. (a) 4-buoy layout in Perth, power=399474 (Watt), (b) Sydney wave model, power=405943 (Watt). The order of the placed and modified buoys position are numbered.

model to interactions between just 4 buoys makes these evaluations very fast and efficient. Figure 1 shows the detailed behaviour of this step.

- **Second step:** Discretising the search space (wave farm) based on the size of the surrogate sub-layout model as a smart initialisation method. Thus composing a large wave farm as a mosaic of the small surrogate sub-layouts that produce the most energy.
- **Third step:** Generating the initial population with a sufficient number of well-arranged 4-buoy sub-layouts (smart initialisation) and then encoding to binary representation in preparation for running binary GAs on WEC positions.
- **Fourth step:** Applying discrete optimisation methods on binary representations. We evaluate and compare the performance of three methods (bDE [22], bGA [21] and bPSO [23]).
- **Fifth step:** if the improvement rate of the last populations of the applied optimisation method is low, the rotate procedure is run to perturb sub-layouts and avoid premature convergence. The rotate algorithm mutates a 4-buoy sub-layout by a random clockwise rotation degree with discrete 45° intervals.

The probability of the applied rotation on each sub-layout is $\frac{1}{N}$.

Using this configurable method, we compare three combinations:

1. SLS-NM + binary GA + Rotate (SLSNM-bGA)
2. SLS-NM + Improved binary DE + Rotate (SLSNM-bDE)
3. SLS-NM + Enhanced binary PSO + Rotate (SLSNM-bPSO)

5.4 Hybrid Multi-strategy Evolutionary algorithms

The binary-encoded search space in the third hybrid search strategy is discrete. This means that, often, there is still scope to further tune layout locations. To implement this tuning we develop the third hybrid search strategy using a backtracking method for enhancing the buoys position. This backtracking idea is consists of

1. A discrete local search (DLS) for providing a second chance for running a fast neighbourhood exploration of the buoys with a large step size (interval=50m)
2. and a continuous local search (CLS) that uses a 1+1EA for exploring near each buoy using small random normally distributed step size ($\sigma = 20m$, linearly decreased).

Furthermore, the rotation procedure is embedded with the discrete metaheuristic algorithms as a mutation operator which is applied to perturb the best solution after each generation. According to the above descriptions, three Hybrid Multi-strategy Evolutionary algorithms are proposed including

1. SLS-NM + bGA-Rotate + DLS + CLS (MS-bGA)
2. SLS-NM+Improved bDE-Rotate + DLS + CLS (MS-bDE)
3. SLS-NM+Enhanced bPSO-Rotate + DLS + CLS (MS-bPSO)

Algorithm 1 describes MS-bDE in detail, where N , N_s , N_b are the buoy numbers, the surrogate model's buoy number (4-buoy layout) and the number of binary decision variables respectively. And also both Tr_1 and Tr_2 are the stopping criteria of 24 (hours) and 48 (hours) respectively.

6 Experimental study

This section shows detailed optimisation results comparing the 17 variations of search heuristics (six existing methods with and 11 new combinations) described in the previous section. In order to evaluate the performance of the proposed algorithms, we performed a comparative study using two distinct real wave scenarios (Perth and Sydney), and for two different large farm sizes with $N = 49$ and $N = 100$ buoys. For each optimisation method with the configurations above, we execute ten runs. For a set of runs, we tracked performance distributions, and the best layouts were gathered to compare each method.

Table 1 shows summary statistics from the experimental runs. The best-obtained results are indicated in bold type. The minimum, maximum, average, median and standard deviation (STD) of the best-produced solutions (power output) for each experiment are reported.

Algorithm 1 *MS – bDE*

```

1: procedure HYBRID MULTI-STRATEGY EVOLUTIONARY ALGORITHM
2: Initialisation
3:  $N = 49, 100, N_s = 4, N_b = N/N_s, N_{Pop} = 12, F_0 = 0.5, P_{cr} = 0.9, iter = 1$ 
4:  $size = \sqrt{N} * 20000$  ▷ Farm size
5:  $\vec{S}_s = \{\langle x_1, y_1 \rangle, \dots, \langle x_{N_s}, y_{N_s} \rangle\} = \perp$  ▷ Continuous surrogate position
6:  $\vec{S} = \{\langle x_1, y_1 \rangle, \dots, \langle x_N, y_N \rangle\} = \perp$  ▷ Discrete layout position
7:  $\chi_{dis} = \{\langle \vec{S}_1 \rangle, \langle \vec{S}_2 \rangle \dots, \langle \vec{S}_{N_{Pop}} \rangle\}$  ▷ Discrete Population
8: Symmetric Local Search + Nelder-Mead (SLS-NM)
9:  $(energy_s, Array_s) = \text{SLS} - \text{NM}([\vec{S}_s])$  ▷ Optimise surrogate model
10:  $\chi_{dis}^{iter} = \text{IniFirstPop}(Array_s, \chi_{dis})$  ▷ Generate initial discrete population
11:  $(Energy, bestEnergy, bestArray) = \text{Eval}(\chi_{dis}^{iter})$  ▷ Evaluate population
12:  $\chi_b^{iter} = \text{ConDisBin}(\chi_{dis}^{iter}, N_b)$  ▷ Encode discrete to binary population
13: Discrete Differential Evolution (bDE)
14: while  $ImPorate \geq 0.1\% \ \& \ \sum_{t=1}^{iter} runtime_t \leq Tr_1$  do
15:   for  $i$  in  $[1, \dots, N_{Pop}]$  do ▷ Mutation
16:     Generate two rand indexes  $r_1, r_2 \in (1, N_{Pop}), r_1 \neq r_2 \neq i$ 
17:     Compute mutant vector  $(V_i^{iter})$  by Equations. 6 and 7
18:     for  $j$  in  $[1, \dots, N_b]$  do ▷ Crossover
19:       if  $rand \leq P_{cr}$  or  $j == j_{rand}$  then
20:          $U_{i,j}^{iter} = V_{i,j}^{iter}$ 
21:       else
22:          $U_{i,j}^{iter} = \chi_{b_{i,j}}^{iter}$ 
23:       end if
24:     end for
25:     if  $f(U_i^{iter}) \geq f(\chi_{b_i}^{iter})$  then ▷ Selection(Maximisation)
26:        $\chi_{b_i}^{iter+1} = U_i^{iter}$ 
27:     else
28:        $\chi_{b_i}^{iter+1} = \chi_{b_i}^{iter}$ 
29:     end if
30:   end for
31:    $(bestarray, bestIndex, bestEnergy, ImPorate) = \text{Max}(\chi_b^{iter+1})$ 
32: Rotation Operator
33:   for  $k$  in  $[1, \dots, N_b]$  do
34:     if  $rand < \frac{1}{N_b}$  then
35:        $(array_{R_k}) = \text{Rotate}(bestarray, k)$ 
36:     end if
37:   end for
38:    $(Energy_R) = \text{Eval}(array_R)$  ▷ Evaluate rotated layout
39:    $\chi_{b_{bestIndex}}^{iter+1} = \begin{cases} array_R, & \text{if } Energy_R > bestEnergy \\ bestarray, & \text{Otherwise} \end{cases}$ 
40:    $iter = iter + 1$ , and Update  $ImPorate$ 
41: end while
42:  $(bestarray, bestIndex, bestEnergy, ImPorate) = \text{Max}(\chi_b^{iter})$ 
43: Discrete Local Search
44: while  $ImPorate \geq 0.001\% \ \& \ \sum_{t=1}^{iter} runtime_t \leq Tr_2$  do
45:    $(array_{dls}, Energy_{dls}) = \text{DLS}(bestarray)$ 
46:   if  $Energy_{dls} > bestEnergy$  then
47:      $bestarray = array_{dls}$ 
48:      $bestEnergy = Energy_{dls}$ 
49:     Update  $ImPorate$ 
50:   end if
51: end while
52: Continuous Local Search
53: while  $\sum_{t=1}^{iter} runtime_t \leq 72(\text{hour})$  do
54:    $(array_{cls}, Energy_{cls}) = \text{CLS}(bestarray)$ 
55:    $bestarray = \begin{cases} array_{cls}, & \text{if } Energy_{cls} > bestEnergy \\ bestarray, & \text{Otherwise} \end{cases}$ 
56:   Update  $bestEnergy$ 
57: end while
58: return  $bestarray, bestEnergy$  ▷ Final Layout and Energy
59: end procedure

```

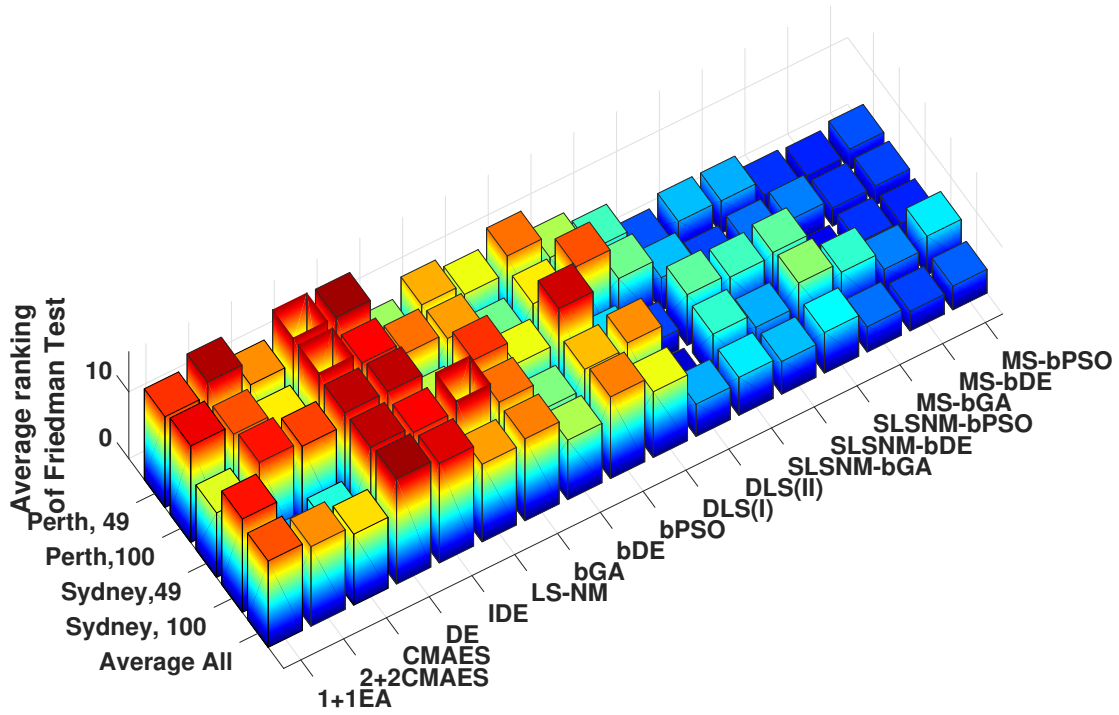


Figure 2: Average ranking of the Friedman test for performance of the proposed optimisation methods. Among all applied heuristic methods, MS-bDE achieves the best average rank in both wave scenarios and wave farm sizes (2.96).

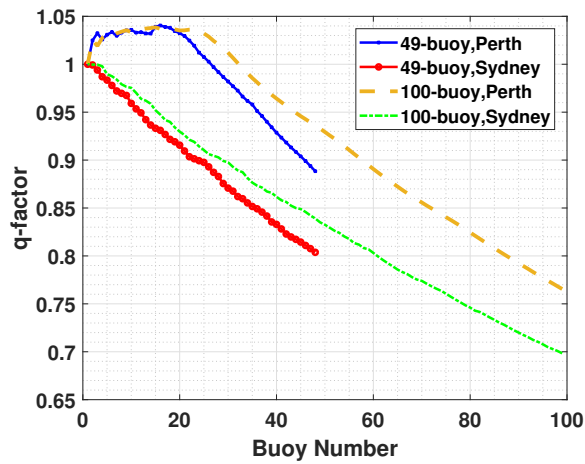


Figure 3: Evaluation of the q-factor performance of the best 49 and 100-buoy layouts by iteratively removing the buoy with the lowest produced power.

In the Perth wave scenario, the best 49 and 100-buoy layouts are found by MS-bDE. However, we can see the MS-bGA and DLS perform better than other optimisation methods in the Sydney wave regime for 49 and 100-buoy layouts, respectively.

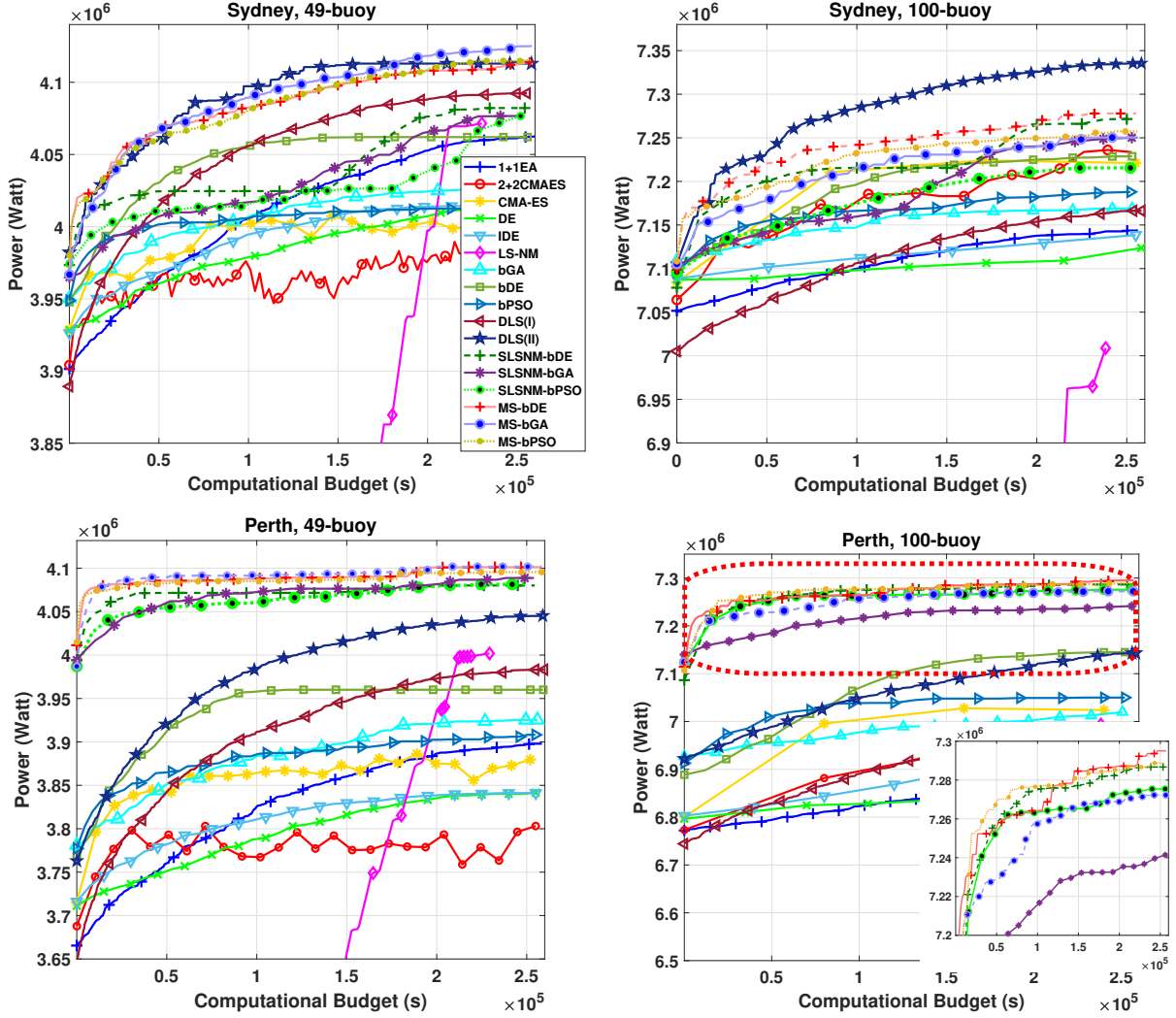


Figure 4: Evolution and convergence rate of the average power output of the 17 algorithms for two real wave models. A zoomed version of the plots is provided to give a better view of convergence speed of the new proposed algorithms.

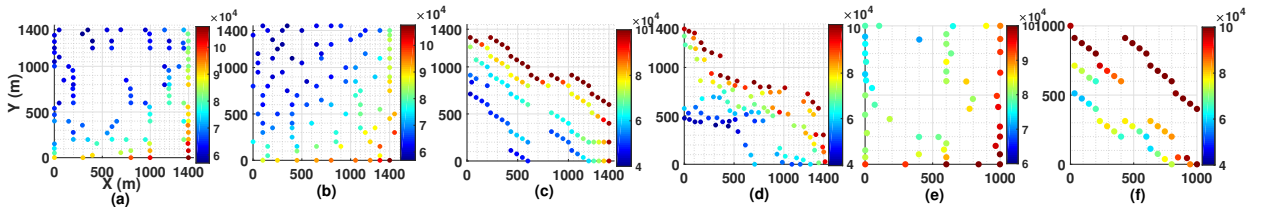


Figure 5: The best 49 and 100-buoy layouts: (a) Power=7337922 (Watt), q-factor=0.7 by MS-bDE for 100-buoy in Sydney wave scenario; (b) Power=7362279 (Watt), q-factor=0.70 for 100-buoy in Sydney wave farm ; (c) Power=7347403 (Watt), q-factor=0.76 by MS-bDE for 100-buoy in Perth wave farm; (d) Power=7235425 (Watt), q-factor=0.75 by LS-NM for 100-buoy in Perth; (e) Power=4145252 (Watt), q-factor=0.80 by MS-bGA for 49-buoy in Sydney ; (f) Power=4177658 (Watt), q-factor=0.88 by MS-bDE for 49-buoy in Perth wave farm (2.4% more power than LS-NM best 49-buoy layout).

Table 1: A performance comparison of the tested heuristics for the 49 and 100-buoy cases, based on maximum, minimum, median and mean power output layout of the best solution per experiment.

Perth wave scenario (49-buoy)																	
	I+1EA	2+2CMAES	CMAES	DE	IDE	LS-NM	bGA	bDE	bPSO	DL(SI)	DL(SII)	SLSNM-bGA	SLSNM-bDE	SLSNM-bPSO	MS-bGA	MS-bDE	MS-bPSO
Max	3933532	3863159	3946189	3860444	3875783	4080796	3984477	4010788	3951612	4029731	4075129	4112549	4097756	4112602	4143453	4177659	4153355
Min	3822270	3819043	3900198	3817360	3774422	3870593	3884613	3914666	3889598	3916594	4034768	4071398	4055033	4082473	4080411	4108205	4081240
Mean	3897954	3847996	3920466	3841577	3841125	4001900	3925487	3960060	3912453	3984165	4045675	4092000	4080173	4082473	4101887	4101260	4095598
Median	3904627	3853485	3923422	3842720	3848962	4008882	3919409	3964299	3912960	3987689	4044025	4090929	4081414	4082183	4099826	4095057	4089500
Std	32160	14659	17904	13118	26134	57673	30027	27647	17177	33047	10639	10535	14291	12556	15447	33245	19794
Perth wave scenario (100-buoy)																	
	I+1EA	2+2CMAES	CMAES	DE	IDE	LS-NM	bGA	bDE	bPSO	DL(SI)	DL(SII)	SLSNM-bGA	SLSNM-bDE	SLSNM-bPSO	MS-bGA	MS-bDE	MS-bPSO
Max	6949622	7159987	7106268	6884148	7071418	7235426	7069638	7205581	7115011	7147428	7192402	7293928	7334975	7317723	7337150	7347403	7323919
Min	6869548	6893283	6840548	6822275	6830504	6522058	6974571	7031121	7001017	6881014	7096030	7198081	7185982	7201029	7209405	7240886	7233752
Mean	6909165	6976394	7038973	6841196	6936048	6926550	7019850	7145057	7050040	6982706	7144278	7252075	7286727	7275411	7272215	7293645	7287221
Median	6908770	6931793	7058938	6834645	6912788	6888912	7017830	7160194	7036276	6978218	7143539	7250198	7294572	7276700	7259815	7287454	7286829
Std	23522	101719	68757	19143	80329	213896	28773	46510	33182	74593	29736	26291	40569	30945	48338	30656	23286
Sydney wave scenario (49-buoy)																	
	I+1EA	2+2CMAES	CMAES	DE	IDE	LS-NM	bGA	bDE	bPSO	DL(SI)	DL(SII)	SLSNM-bGA	SLSNM-bDE	SLSNM-bPSO	MS-bGA	MS-bDE	MS-bPSO
Max	4082524	4036152	4061528	4028337	4062984	4089731	4052984	4078389	4036728	4108751	4134622	4105401	4100089	4084955	4145252	4132385	4125968
Min	4046311	4013471	4015919	4002550	3976301	4039525	4006283	4050349	3992467	4070321	4098276	4031291	4047364	4066979	4106192	4097087	4107365
Mean	4062828	4026230	4029509	4014852	4014611	4063963	4028394	4062048	4015029	4092373	4116149	4075606	4082176	4076665	4125113	4113961	4117115
Median	4060505	4029230	4030342	4015482	4011081	4064273	4025310	4059954	4015661	4095077	4113040	4072725	4083311	4076621	4127949	4113672	4117134
Std	9580	7808	12500	8591	20268	18106	13725	7924	11643	10140	10814	19897	13306	4946	12113	9324	5856
Sydney wave scenario (100-buoy)																	
	I+1EA	2+2CMAES	CMAES	DE	IDE	LS-NM	bGA	bDE	bPSO	DL(SI)	DL(SII)	SLSNM-bGA	SLSNM-bDE	SLSNM-bPSO	MS-bGA	MS-bDE	MS-bPSO
Max	7143849	7325364	7292118	7179529	7195009	7182442	7209740	7285926	7229868	7246878	7362279	7288882	7338191	7290958	7300092	7337922	7309508
Min	7117313	7225156	7088371	7094498	7114283	6770261	7128255	7132653	7159246	7048150	7307167	7210217	7240062	7167618	7209436	7247446	7203600
Mean	7143849	7268166	7242833	7123588	7138670	7008764	7168951	7228751	7187912	7166332	7335497	7246161	7271553	7228570	7250348	7277918	7257887
Median	7140541	7263653	7266642	7121216	7132516	7025996	7164768	7236813	7183483	7172586	7339777	7245065	7267610	7237676	7233001	7274685	725276
Std	18069	34055	64716	24211	25094	131454	25026	41309	20879	57189	18211	22690	31592	42732	32945	26909	33889

In addition, Figure 2 depicts a broad comparison of all proposed optimisation methods by the average ranking of the non-parametric Friedman’s test [25] including both real wave scenarios with two different farm sizes and the total average rank of each method in all case studies. It can be seen that, overall, MS-bDE produces the best optimisation performance.

In Figure 4, in all configurations of the Perth wave model, three hybrid and three multi-strategy methods converge very fast and still outperform the other methods. It is notable that these six proposed methods start the optimisation process with a high power output solution due to the smart initialisation technique described in Section 5.3. Looking more closely at Figure 4, we can see that all discrete optimisation approaches converge faster than the continuous algorithms on average. Furthermore, because of the embedding of the rotation operator with the binary EAs, the multi-strategy techniques are able to converge faster than the hybrid methods, especially in the initial iterations. In terms of other algorithms, in the Sydney wave model, the performance of the DLS is strong ($N = 100$) and outperforms other methods in terms of the convergence rate and the produced power. However, we can see that in the smaller farm, the performance of multi-strategy EAs are competitive, and MS-bGA performs better than other optimisation methods in the final iterations.

Some of the most productive 49 and 100-buoy layouts are presented by Figure 5 from all the runs in the two scenarios. The absorbed power of buoys is characterised by their colour. It can be seen that the best layouts in Perth are multi-row diagonal arrangements; however, this trend is different in the Sydney wave site where the optimisation method pushes some buoys to the farm boundaries.

Lastly, to further investigate the hydrodynamic interactions between buoys in the best layouts, we perform two different analyses.

In the first analysis, we iteratively remove the buoy with the lowest absorbed power and evaluate the performance of the layout. While this experiment focuses on the least-performing buoy, the interactions of these buoys might be beneficial for the wave farms nevertheless. Figure 3 shows that a lot of constructive interference is exploited in both the 49 and 100 buoy Perth scenario (up to the 26th buoy), while the marginal improvement from adding buoy’s declines after that. For Sydney, there is an almost uniform decline in marginal performance from the start.

The second analysis of the best layouts selects the buoy with the highest power, removes it, and then maps the landscape using a 25-meter grid. We record both the absorbed power of the buoy and the total wave farm power output per each sample. Figure 6 shows the power landscape analysis of this experiment.

Note that the gaps are the infeasible areas around the already-placed buoys. The subplots (b) and (d) indicate a multimodal and complex power landscape, for the placement of the last of the 49 buoys, especially for Sydney.

In order to report on the distribution of the performance of the different approaches across 10 independent runs, the box-plots (Figure 7) is represented. Figure 7 shows and highlights the considerable performance of the proposed multi-strategy optimisation framework compared with other optimisation techniques in the large wave farms problem.

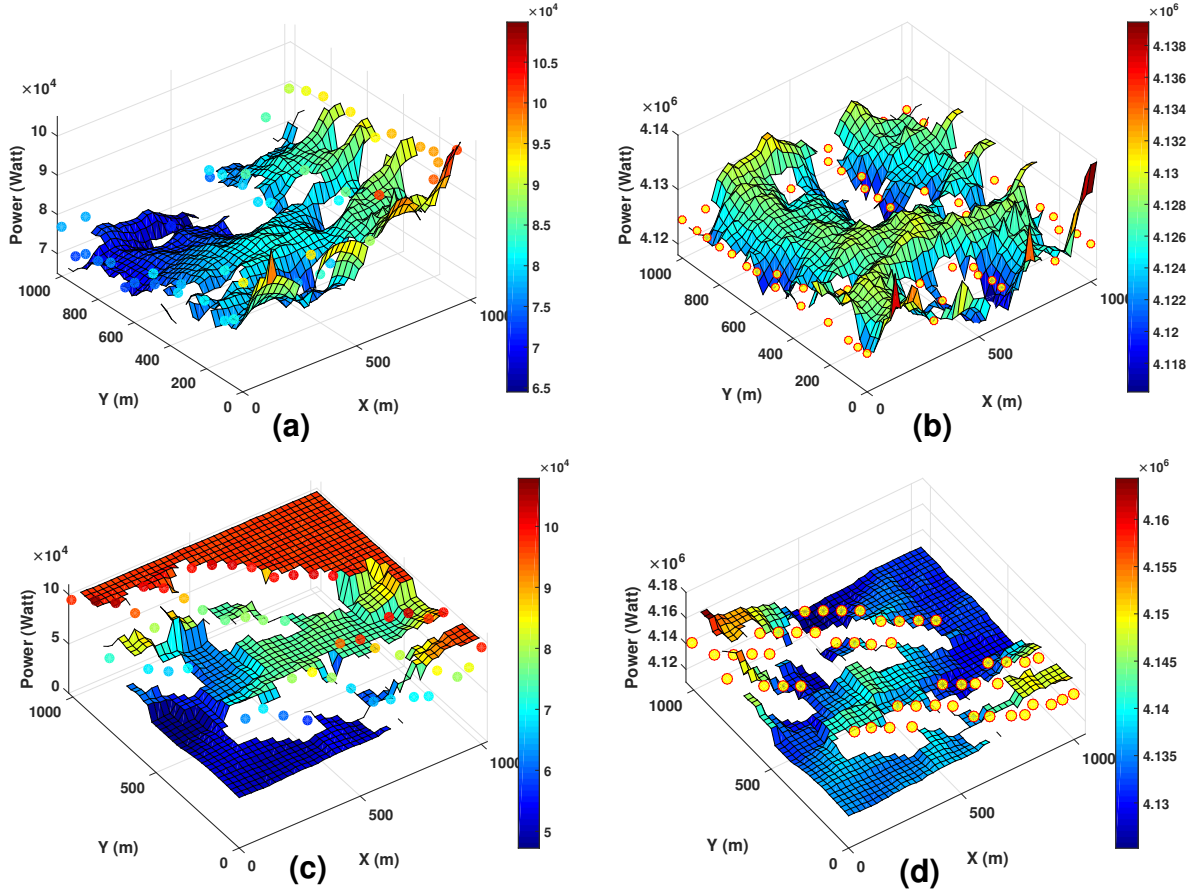


Figure 6: Power landscape analysis of the best 49-buoy layouts. (a) Sydney - wave state - grid sampling the power extracted by the final buoy. (b) Sydney, *total* energy extracted with grid sampling of the final buoy position (c) Perth-wave state - grid sampling of last buoy's power. (d) grid sampling of total power w.r.t last buoy's position. No samples are made within the safe distance of already-placed buoys. The power of each buoy is characterised by a specific colour in both (a) and (c).

Meanwhile, All implemented codes and auxiliary materials are publicly available: <https://cs.adelaide.edu.au/~optlog/research/energy.php>.

7 Conclusions

In this paper, we have proposed, assessed, and systematically compared 17 different optimisation approaches for optimising the arrangement of large wave farms with 49 and 100 generators in two real wave regimes (Sydney and Perth). This study comprised three new hybrid algorithms, each with three variants as a multi-strategy EA framework customised to this field.

This optimisation problem is challenging in terms of the cost of its evaluation model and the large multimodal search landscape. Our new framework addresses this problem through careful problem decomposition into sub-farms, the use of discrete search spaces and a customised mutation operator (rotation).

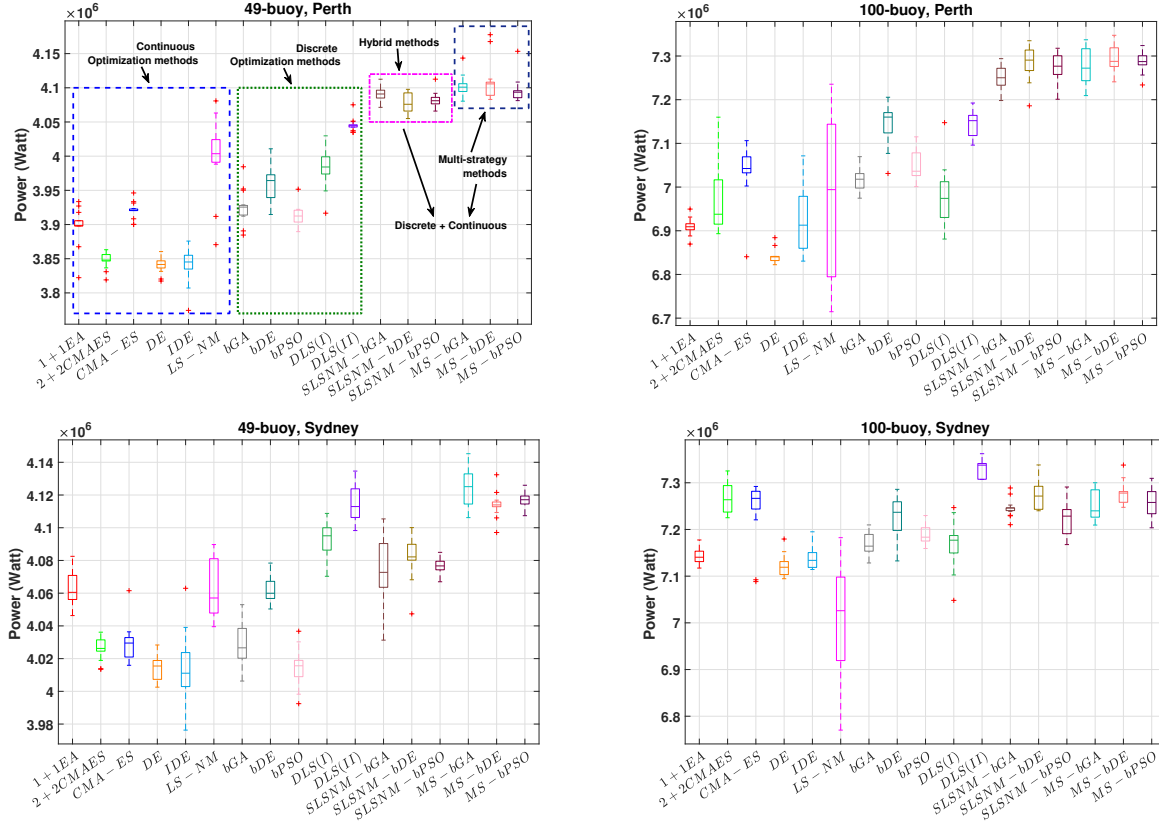


Figure 7: The comparison of the optimisation algorithms performance for 49 and 100-buoy layouts in Sydney and Perth wave models. The optimisation results present the best solution per each experiment. (10 independent runs per each method)

The statistical results indicate that the new multi-strategy evolutionary algorithm consisting of symmetric local search and Nelder Mead search, combined with an embedded rotation operator, plus an improved binary DE and a hybrid backtracking strategy (DLS+CLS) performs better than other applied optimisation methods on average. In our experiments, this method overcomes other state-of-the-art algorithms, for both 49 and 100-buoy layouts, in terms of convergence speed and power production.

Future work could explore other optimisation dimensions, including considering other effective buoy designs and power take-off system settings.

Acknowledgements

We would like to offer our special thanks to Dr.Hansen, Dr.kalami and Dr.Mirjalili for sharing and publishing their valuable source codes and also thank Mr.Roostapour for his good comments. Additionally, This research is supported with supercomputing resources provided by the Phoenix HPC service at the University of Adelaide.

References

- [1] Matthias Kimmel Bryony Collins Albert Cheung Lisa Becker Rohan Boyle, David Strahan et al. Global trends in renewable energy investment 2019. *United Nations Environment Programme*, 2019.
- [2] B Drew, A R Plummer, and M N Sahinkaya. A review of wave energy converter technology. *Proceedings of the Institution of Mechanical Engineers, Part A: Journal of Power and Energy*, 223(8):887–902, 2009.
- [3] Diego Vicinanza, Jørgen Harck Nørgaard, Pasquale Contestabile, and Thomas Lykke Andersen. Wave loadings acting on overtopping breakwater for energy conversion. *Journal of Coastal Research*, 65(sp2):1669–1674, 2013.
- [4] Nataliia Y Sergiienko, Mehdi Neshat, Leandro SP da Silva, Bradley Alexander, and Markus Wagner. Design optimisation of a multi-mode wave energy converter. *arXiv preprint arXiv:2001.08966*, pages 1–19, 2020.
- [5] L Cuadra, S Salcedo-Sanz, JC Nieto-Borge, E Alexandre, and G Rodríguez. Computational intelligence in wave energy: Comprehensive review and case study. *Renewable and Sustainable Energy Reviews*, 58:1223–1246, 2016.
- [6] A. D. De Andrés, R. Guanche, L. Meneses, C. Vidal, and I. J. Losada. Factors that influence array layout on wave energy farms. *Ocean Engineering*, 82:32–41, 2014.
- [7] B. F. M. Child and Vengatesan Venugopal. Optimal configurations of wave energy device arrays. *Ocean Engineering*, 37(16):1402–1417, 2010.
- [8] P. Ruiz, V. Nava, M. B. R. Topper, P. R. Minguela, F. Ferri, and J. P. Kofoed. Layout optimisation of wave energy converter arrays. *Energies*, 10(9):1262, 2017.
- [9] J. Wu, S. Shekh, N. Y. Sergiienko, B. S. Cazzolato, B. Ding, F. Neumann, and M. Wagner. Fast and effective optimisation of arrays of submerged wave energy converters. In *Genetic and Evolutionary Computation Conference (GECCO)*, pages 1045–1052. ACM, 2016.
- [10] M. Neshat, B. Alexander, M. Wagner, and Y. Xia. A detailed comparison of meta-heuristic methods for optimising wave energy converter placements. In *Genetic and Evolutionary Computation Conference (GECCO)*, pages 1318–1325. ACM, 2018.
- [11] Mehdi Neshat, Bradley Alexander, Nataliia Sergiienko, and Markus Wagner. A new insight into the position optimization of wave energy converters by a hybrid local search. *arXiv preprint arXiv:1904.09599*, 2019.
- [12] N. Hansen. The cma evolution strategy: a comparing review. *Towards a new evolutionary computation*, pages 75–102, 2006.
- [13] K. N. Krishnanand and D. Ghose. Glowworm swarm optimization for simultaneous capture of multiple local optima of multimodal functions. *Swarm Intelligence*, 3(2):87–124, 2009.
- [14] Mehdi Neshat, Bradley Alexander, Nataliia Y Sergiienko, and Markus Wagner. A hybrid evolutionary algorithm framework for optimising power take off and placements of wave energy converters. In *Proceedings of the Genetic and Evolutionary Computation Conference*, pages 1293–1301. ACM, 2019.

- [15] Mehdi Neshat, Ehsan Abbasnejad, Qinfeng Shi, Bradley Alexander, and Markus Wagner. Adaptive neuro-surrogate-based optimisation method for wave energy converters placement optimisation. In *International Conference on Neural Information Processing*, pages 353–366. Springer, 2019.
- [16] L. D. Mann, A. R. Burns, , and M. E. Ottaviano. Ceto, a carbon free wave power energy provider of the future. In *the 7th European Wave and Tidal Energy Conference (EWTEC)*, 2007.
- [17] N. Y. Sergiienko. Wave energy converter (wec) array simulator (<https://www.mathworks.com/matlabcentral/fileexchange/71840-wave-energy-converter-wec-array-simulator>), 2020. Retrieved February 6, 2020.
- [18] Nikolaus Hansen. Cma-es: Evolution strategy with covariance matrix adaptation for nonlinear function minimization (<http://www.lri.fr/hansen/purecmaes.m>), 2009. Retrieved March 20, 2018.
- [19] R. Storn and K. Price. Differential evolution—a simple and efficient heuristic for global optimization over continuous spaces. *Journal of global optimization*, 11(4):341–359, 1997.
- [20] Hong-Wei Fang, Yu-Zhu Feng, and Guo-Ping Li. Optimization of wave energy converter arrays by an improved differential evolution algorithm. *Energies*, 11(12):3522, 2018.
- [21] C. Sharp and B. DuPont. Wave energy converter array optimization: A genetic algorithm approach and minimum separation distance study. *Ocean Engineering*, 163:148–156, 2018.
- [22] Ezgi Zorarpacı and Selma Ayşe Özel. A hybrid approach of differential evolution and artificial bee colony for feature selection. *Expert Systems with Applications*, 62:91–103, 2016.
- [23] Seyedali Mirjalili and Andrew Lewis. S-shaped versus v-shaped transfer functions for binary particle swarm optimization. *Swarm and Evolutionary Computation*, 9:1–14, 2013.
- [24] Seyedali Mirjalili. Enhanced binary particle swarm optimization (bpsi) with 6 new transfer functions (<https://www.mathworks.com/matlabcentral/fileexchange/42448-enhanced-binary-particle-swarm-optimization-bpsi-with-6-new-transfer-functions>), 2020. Retrieved March 21, 2020.
- [25] Myles Hollander, Douglas A Wolfe, and Eric Chicken. *Nonparametric statistical methods*, volume 751. John Wiley & Sons, 2013.